



# PCSK9 inhibitor inclisiran for treating atherosclerosis via regulation of endothelial cell pyroptosis

Ni Kong<sup>1</sup>, Qin Xu<sup>1</sup>, Wei Cui<sup>2</sup>, Xiaoying Feng<sup>3</sup>, Huijie Gao<sup>4</sup>

<sup>1</sup>School of Pharmacy, Naval Medical University, Shanghai, China; <sup>2</sup>Basic Medical School, Qingdao University, Qingdao, China; <sup>3</sup>School of Pharmacy, Guangzhou Medical University, Guangzhou, China; <sup>4</sup>Department of Immunopharmacology, Jining Medical University, Rizhao, China

**Contributions:** (I) Conception and design: N Kong; (II) Administrative support: N Kong; (III) Provision of study materials or patients: N Kong, Q Xu, W Cui; (IV) Collection and assembly of data: X Feng, H Gao; (V) Data analysis and interpretation: H Gao; (VI) Manuscript writing: All authors; (VII) Final approval of manuscript: All authors.

**Correspondence to:** Huijie Gao. Department of Immunopharmacology, Jining Medical University, No. 669, Xueyuan Road, Donggang District, Rizhao, China. Email: gaohuijie2019@163.com; Ni Kong. School of Pharmacy, Naval Medical University, No. 325, Guohe Road, Yangpu District, Shanghai, China. Email: koni69689@tom.com or Kongni0113@163.com.

**Background:** Proprotein convertase subtilisin/kexin type 9 (PCSK9) belongs to an intracellular invertase or decarboxylase and is an independent risk factor for atherosclerosis (AS). This study aimed to investigate the therapeutic potential of the PCSK9 inhibitor, inclisiran, and its underlying mechanism in AS.

**Methods:** ApoE<sup>-/-</sup> mice were fed with a high-fat diet (HFD) and intraperitoneally injected with 1, 5, or 10 mg/kg inclisiran. Low-density lipoprotein cholesterol (LDL-C), total cholesterol (TC), triglyceride (TG), and high-density lipoprotein cholesterol (HDL-C) levels were determined using commercially available kits. Oil Red O staining was applied to detect the aortic plaque area and oil formation. Human umbilical vein endothelial cells (HUVECs) were treated with oxidized low-density lipoprotein (ox-LDL) to induce cell injuries. Cell death was determined using a Hoechst 33342/propidium iodide (PI) dual-staining assay. Cytotoxicity was measured by lactate dehydrogenase (LDH) activity analysis. Quantitative real-time polymerase chain reaction (qRT-PCR) and western blot analyses were performed to examine the pyroptosis-related factors.

**Results:** Inclisiran inhibited the levels of LDL-C, TC, and TG, but increased the HDL-C level in the AS animal model. It also significantly inhibited plaque and oil droplet formation in a dose-dependent manner. Moreover, inclisiran markedly inhibited pyroptosis, as evidenced by the decreased levels of cleaved-caspase-1, NOD-like receptor family pyrin domain containing 3 (NLRP3), apoptosis-associated speck-like protein containing a caspase-1 recruitment domain (ASC), gasdermin-D (GSDMD)-N, interleukin (IL)-1 $\beta$ , and IL-18. Furthermore, inclisiran substantially inhibited cell death and cytotoxicity induced by ox-LDL in HUVECs.

**Conclusions:** Inclisiran exerted an anti-atherosclerotic effect by inhibiting pyroptosis. This study provides a theoretical basis for the therapeutic potential of inclisiran in AS.

**Keywords:** Inclisiran; atherosclerosis (AS); pyroptosis; high-fat diet (HFD)

Submitted Aug 22, 2022. Accepted for publication Oct 25, 2022.

doi: 10.21037/atm-22-4652

View this article at: <https://dx.doi.org/10.21037/atm-22-4652>

## Introduction

Atherosclerosis (AS) is a chronic inflammatory disease in which lipids accumulate on arterial walls, resulting in AS and stenosis of the vascular lumen (1). Cardiovascular

diseases induced by AS, such as coronary artery disease, stroke, and peripheral artery disease, are the main causes of high morbidity and mortality in humans (2). Globally, approximately 20 million people die of AS diseases each

year (3). AS manifests primarily as fatty degeneration of the arterial wall and formation of atherosclerotic plaques, leading to lumen narrowing and also causing mechanical dysfunction of the vascular wall (1). The risk factors for AS include hypertension, hyperlipidemia, smoking, diabetes, obesity, and genetic factors (4). At present, the main drugs used for the treatment of AS are lipid-lowering, anticoagulant, and thrombolytic drugs; however, their therapeutic effects are unsatisfactory. Therefore, it is necessary to explore new treatment methods for AS from genetic and molecular perspectives.

Proprotein convertase subtilisin/kexin type 9 (PCSK9) is composed of 692 amino acids encoded by the PCSK9 gene located on chromosome 1p32.3 (5). It belongs to an intracellular invertase or decarboxylase, which is mainly expressed in the liver and intestinal tract and is also slightly expressed in the kidney and brain (5-8). PCSK9 regulates plasma levels of low-density lipoprotein cholesterol (LDL-C), which is an independent risk factor for AS (9,10). Therefore, PCSK9 is the target of AS treatment and plays a unique therapeutic role in AS. Inclisiran, a chemically synthesized small interfering RNA (siRNA) that targets the PCSK9 gene, can significantly reduce LDL-C levels and has superior safety and tolerance (11,12). ORION-10 and ORION-11 (ClinicalTrials.gov numbers, NCT03399370 and NCT03400800), inclisiran's two phase 3 trials, enrolled 1,561 and 1,617 patients with AS-associated cardiovascular disease or AS-associated cardiovascular disease risk equivalent, who administered with inclisiran had reductions in LDL cholesterol levels of approximately 50% (13). In a phase 2 trials, enrolled 501 patients with elevated LDL cholesterol levels at high cardiovascular risk, PCSK9 and LDL cholesterol levels were found to be lowered by inclisiran administration (ORION-1 ClinicalTrials.gov number, NCT02597127) (11). However, the related mechanism of inclisiran in AS needs to be further studied.

First proposed by Cookson in 2001, pyroptosis is a pro-inflammatory, lytic, programmed cell death method that relies on the activation of caspase-1 (14). It is characterized by the formation of pores, rupture of the plasma membrane, and the entry of cell contents and pro-inflammatory mediators into the intercellular substance, leading to inflammation and cell death (15,16). Endothelial cell (EC) pyroptosis releases adhesion, chemotactic, and pro-inflammatory factors, which induce an early arterial inflammatory response, cause local lipid deposition, and promote the formation of AS and plaque instability (17).

Recent studies have indicated that cell pyroptosis plays a vital role in the formation of AS. For example, nicotine has been shown to accelerate AS by regulating cell pyroptosis (18), and salidroside has been found to reduce the formation of AS plaques by inhibiting EC pyroptosis (19). The present study aimed to investigate the therapeutic potential of the PCSK9 inhibitor, inclisiran, and explore its underlying mechanism *in vivo* and *in vitro*. We present the following article in accordance with the ARRIVE reporting checklist (available at <https://atm.amegroups.com/article/view/10.21037/atm-22-4652/rc>).

## Methods

### Animals

A total of 40 male ApoE<sup>-/-</sup> mice (aged 8 weeks, 17–20 g) were purchased from Jinan Pengyue Laboratory Animal Co., Ltd. (Jinan, China). A protocol was prepared before the study without registration. The mice were fed in specific pathogen-free (SPF) stage rooms at 22±2 °C, 40% humidity, and a 12/12-h light/dark cycle. The animal experiments were performed according to the guidelines of the Chinese Ethics Committee for the care and use of animal research and were approved by the Animal Care and Use Committee of Naval Medical University (No. SCXK2021-0910).

### AS model and inclisiran treatment

The mice were randomly divided into five groups. Random numbers were generated using the standard = RAND() function in Microsoft Excel (Microsoft, Redmond, WA, USA) (20). Staffs and participants were blinded to the randomization. The chow group (n=8) mice were fed with routine chow; the high-fat diet (HFD) group (n=8) mice were fed with HFD; the 1 mg/kg group (n=8) mice were fed with HFD and intraperitoneally injected with 1 mg/kg inclisiran simultaneously; the 5 mg/kg group (n=8) mice were fed with HFD and intraperitoneally injected with 5 mg/kg inclisiran simultaneously; the 10 mg/kg group (n=8) mice were fed with HFD and intraperitoneally injected with 10 mg/kg inclisiran simultaneously. Inclisiran purchased from MedChemExpress (Monmouth Junction, NJ, USA) was dissolved in phosphate buffer saline (PBS) for use in intraperitoneal injection. After 20 weeks, all mice were euthanized using pentobarbital sodium (150 mg/kg) and their aortas and blood specimens were collected.

**Table 1** Primer sequences used for qPCR amplification

Gene	Primer sequences
Mouse <i>NLRP3</i>	Forward: 5'-GGGAGACCGTGAGGAAAGGA-3' Reverse: 5'-CCAAAGAGGAATCGGACA ACAA-3'
Mouse <i>ASC</i>	Forward, 5'-GTGTTTACTCTCTGGGATGTTTTG-3' Reverse: 5'-GTCTGTGGA ATTAGTGTTGGA-3'
Mouse <i>GSDMD</i>	Forward: 5'-CAGAACCGGAGT GTTTTGGC-3' Reverse: 5'-CCCTTGCCTTACCCTTCAA-3'
Mouse <i>IL-1<math>\beta</math></i>	Forward: 5'-CCTCGTGCTGTCGGACCCATA-3' Reverse: 5'-CAGGCTTGTGCTCTGCTTGTGA-3'
Mouse <i>IL-18</i>	Forward: 5'-CCCTTTGAGGCATCCAGGAC-3' Reverse: 5'-GGGGTTCACCTGGCACTTTGA-3'
Mouse <i><math>\beta</math>-actin</i>	Forward: 5'-CCAGCCTCCTTC TTGGGTAT-3' Reverse: 5'-GGGTGTAACGCAGCTCAG-3'
Human <i>NLRP3</i>	Forward: 5'-CTGGCATCTGGGGAAACCT-3' Reverse: 5'-TCTGTGTACAAGGCTCAC-3'
Human <i>ASC</i>	Forward: 5'-TCTACCTGGAGACCTACGGC-3' Reverse: 5'-TCCAGAGCCCTGGTGC-3'
Human <i>GSDMD</i>	Forward: 5'-CTCGCCGACTTCCGTAACCT-3' Reverse: 5'-TGCAGCCACAATAACTCAGC-3'
Human <i>IL-1<math>\beta</math></i>	Forward: 5'-TTCGAGGCACAAGGCACAA-3' Reverse: 5'-TGGCTGCTTCAAGCACTTGA-3'
Human <i>IL-18</i>	Forward: 5'-ATCGCTTCTCTCGCAACAA-3' Reverse: 5'-GTCCGGGTGCATTATCTCT-3'
Human <i><math>\beta</math>-actin</i>	Forward: 5'-GCACAGAGCCTCGCCTTT-3' Reverse: 5'-CACAGGACTCCATGCCAG-3'

qPCR, quantitative polymerase chain reaction.

### Oil red O staining

Arterial sections were stained with oil red O staining for 10–15 min under sealed and dark conditions. The staining will be terminated when red lipid droplets appeared under the microscope (Nikon Corporation, Tokyo, Japan). The sections were differentiated into clear interstitium with 60% ethanol under the microscope. After washing, the nucleus was counterstained with hematoxylin.

### Quantitative real-time polymerase chain reaction (qRT-PCR)

Total RNA was isolated and checked using homogenization with Trizol (Invitrogen, Carlsbad, CA, USA) and the FOTODYNE gel imaging analysis system (Fotodyne,

Inc., Hartland, WI, USA). Complementary DNA (cDNA) was synthesized using a cDNA Cycle Kit (Thermo Fisher Scientific, USA). The primer sequences used for qPCR amplification were listed in *Table 1*. The expression level of  *$\beta$ -actin* was used to standardize the messenger RNA (mRNA) expression, which was calculated by Fold change =  $2^{-\Delta\Delta CT}$ .

### Western blot

Proteins were extracted and quantified using radio immunoprecipitation assay (RIPA) buffer (Biovision, American) and a protein concentration detection kit (absin, Shanghai, China). The prepared protein was separated by polyacrylamide-sodium dodecyl sulfate (SDS) gels and then transferred onto polyvinylidene fluoride (PVDF) membranes (Roche, Switzerland). Next, the membranes were incubated overnight at 4 °C with polyclonal antibodies: cleaved-caspase-1 (#4199T, 1:1,000, Cell Signaling Technology, USA), NOD-like receptor family pyrin domain containing 3 (NLRP3) (ab263899, 1:1,000, Abcam, UK), apoptosis-associated speck-like protein containing a CARD (ASC) (#13833S, 1:1,000, Cell Signaling Technology, USA), gasdermin D (GSDMD)-N (ab215203, 1:1,000, Abcam, UK), interleukin (IL)-1 $\beta$  (ab216995, 1:1,000, Abcam, UK), IL-18 (ab243091, 1:1,000, Abcam, UK), and  $\beta$ -actin (ab8226, 1:1,000, Abcam, UK). After washing with Tris-HCl buffered saline with 0.1% (v/v) Tween 20 (TBST), the membranes were incubated with a secondary antibody, and protein expression intensity was determined by enhanced chemiluminescent (ECL) kit (Beyotime, Beijing, China).

### Biochemical index detection

LDL-C, high-density lipoprotein cholesterol (HDL-C), total cholesterol (TC), and triglyceride (TG) were detected using kits obtained from the Nanjing Jiancheng Biological Engineering Research Institute (Nanjing, China).

### Human umbilical vein endothelial cells (HUVECs) culture

HUVECs (Procell, Wuhan, China) were maintained at 37 °C in a 5% carbon dioxide (CO<sub>2</sub>) humid incubator and cultured in Ham's F-12K medium (Procell) supplemented with 0.1 mg/mL heparin, 0.03 mg/mL EC growth supplements (Procell), and 10% fetal bovine serum (FBS, Gibco, USA).

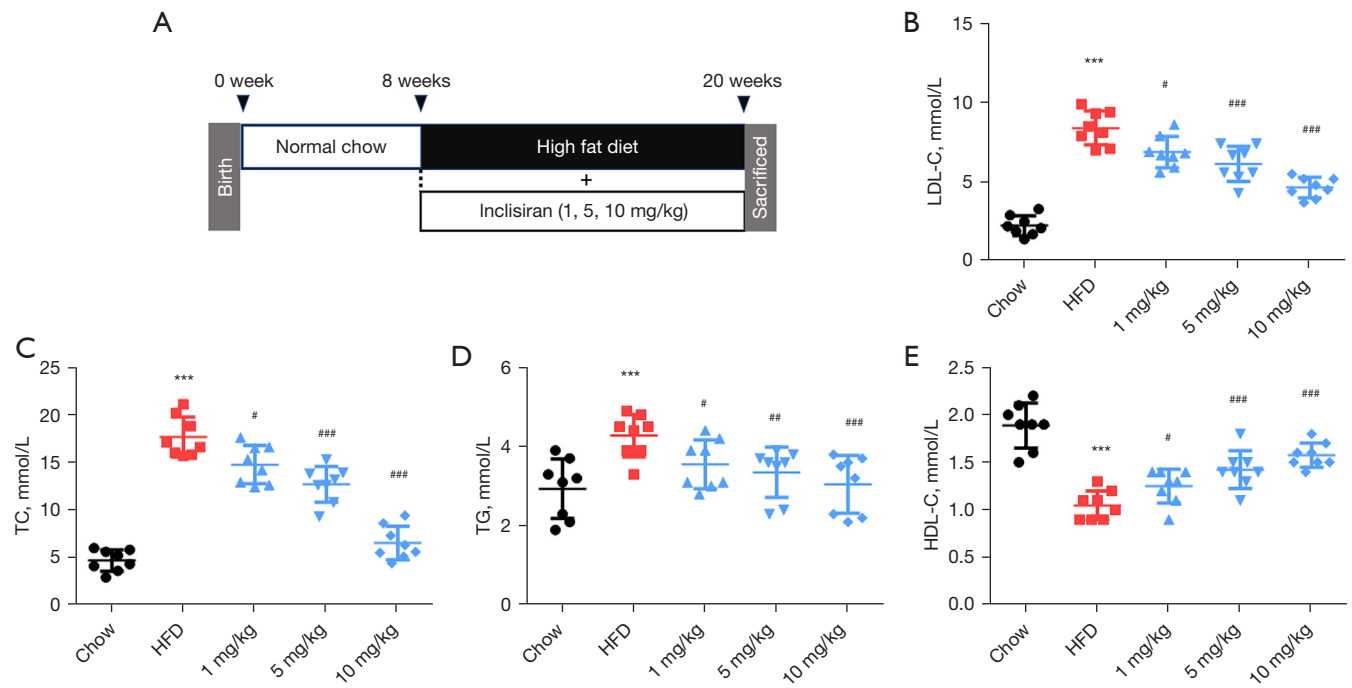


**Figure 1** Inclisiran reduced blood lipids in an AS mouse model. (A) Timeline of ApoE<sup>-/-</sup> mice fed with HFD and treated with inclisiran. Levels of (B) LDL-C, (C) TC, (D) TG, and (E) HDL-C in mice blood were determined using kits. \*\*\*P<0.001 vs. the chow group. #P<0.05, ##P<0.01, and ###P<0.001 vs. the HFD group. LDL-C, low density lipoprotein cholesterol; TC, total cholesterol; TG, triglyceride; HDL-C, high density lipoprotein cholesterol; AS, atherosclerosis; HFD, high-fat diet.

### Oxidized low-density lipoprotein (ox-LDL) stimulation

HUVEC cells were treated with 25 µg/mL ox-LDL for 24 h to induce cell injury and were then treated with different concentrations of inclisiran (50, 100, and 200 nM) for 48 h.

### Hoechst33342 staining

The treated cells were seeded in a six-well plate and stained with 1 mL of hoechst33342 staining solution (Beyotime Biotechnology, Shanghai, China) at room temperature for 25 min. After washing twice with PBS, 1 mL of propidium iodide (PI) staining solution (5 µg/mL, Sigma, USA) was added for 30 min at room temperature. Finally, cell apoptosis was observed and counted under the microscope.

### Lactate dehydrogenase (LDH) level

LDH activity was measured using a Pierce™ LDH Cytotoxicity Assay Kit (ThermoScientific, USA) according to the manufacturer's instructions. A spectrophotometer (Beckman DU800, Fullerton, CA, USA) was used to detect the absorbance at a wavelength of 440 nm.

### Statistical analysis

Data were analyzed by SPSS 21.0 (Chicago, IL, USA). One-way analysis of variance (ANOVA) followed by Tukey's post-hoc test was used to analyze the differences between the groups. P<0.05, P<0.01, and P<0.001 indicated a statistically significant difference between the groups.

## Results

### Inclisiran reduced blood lipids in mice with AS

Normal ApoE<sup>-/-</sup> mice (8 weeks old) were fed with HFD to establish an AS mouse model. As shown in *Figure 1A*, the control group mice were fed with standard chow. Treatment group mice were fed with HFD and injected intraperitoneally with different concentrations of inclisiran (1, 5, and 10 mg/kg). The mice were sacrificed at 20 weeks.

The levels of LDL-C, TC, and TG in the HFD group were higher than that in the chow group, while the level of HDL-C in the HFD group was lower than that in the chow group (P<0.05, *Figure 1B-1E*). Compared with the HFD group, different concentrations of inclisiran significantly

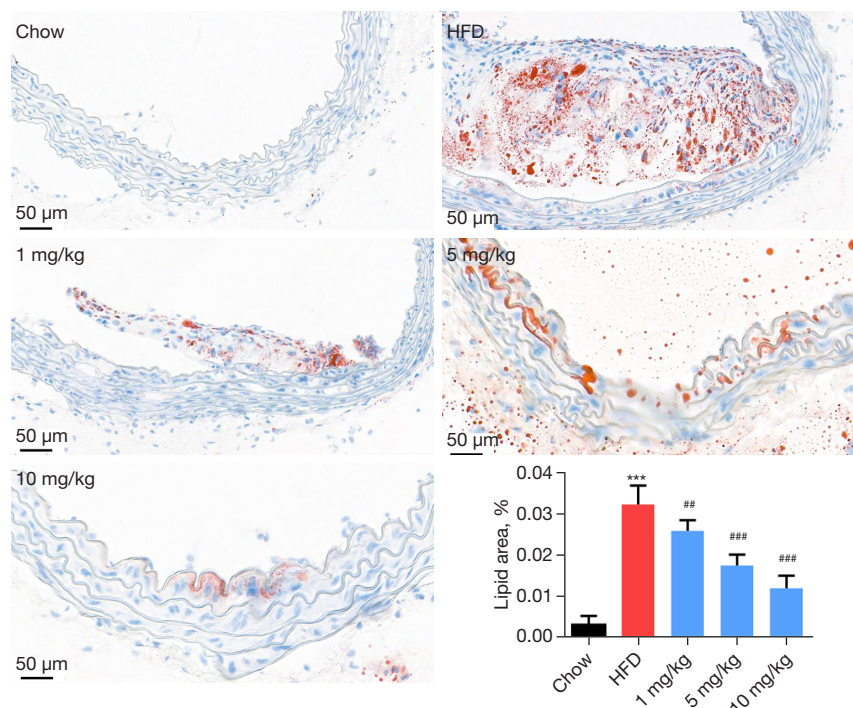


**Figure 2** Inclisiran inhibited the development of AS. Oil Red O staining ( $\times 50$ ) of arterial tissues and the quantitative results.  $***P < 0.001$  vs. the chow group.  $##P < 0.01$  and  $###P < 0.001$  vs. the HFD group. HFD, high-fat diet; AS, atherosclerosis.

inhibited the levels of LDL-C, TC, and TG in a dose-dependent manner ( $P < 0.05$ , *Figure 1B-1D*). Interestingly, compared with the HFD group, different concentrations of inclisiran markedly increased the HDL-C level in a dose-dependent manner ( $P < 0.05$ , *Figure 1E*). Taken together, these results showed that the AS mouse model was established successfully, and inclisiran reduced the blood lipids in AS mice.

#### ***Inclisiran inhibited the development of AS in mice***

The oil red O staining results indicated that compared with the chow group, the HFD groups showed significant oil droplet formation, and obvious AS plaque was observed. Also, compared with the HFD group, different concentrations of inclisiran considerably inhibited oil droplet and AS plaque formation in a dose-dependent manner ( $P < 0.05$ , *Figure 2*).

#### ***Inclisiran inhibited HFD-induced pyroptosis***

The qRT-PCR results showed that the mRNA levels of *NLRP3*, *ASC*, *GSDMD*, *IL-1 $\beta$* , and *IL-18* in the HFD

group were higher than that in the chow group ( $P < 0.05$ , *Figure 3A-3E*). However, these levels were decreased in mice treated with inclisiran relative to those in the HFD group ( $P < 0.05$ ). The western blot results revealed that HFD increased *NLRP3*, *ASC*, *GSDMD-N*, cleaved caspase-1, *IL-1 $\beta$* , and *IL-18* protein levels, while different concentrations of inclisiran significantly inhibited these levels (*Figure 3F*). The above results indicated that inclisiran inhibited HFD-induced pyroptosis.

#### ***Inclisiran inhibited HUVEC cell death induced by ox-LDL***

The Hoechst 33342/PI dual-staining assay was used to detect HUVEC death. As indicated in *Figure 4A, 4B*, PI-positive cells in the ox-LDL group were significantly higher than those in the control group ( $P < 0.05$ ). However, PI-positive cells in the inclisiran-treated groups were markedly reduced in a dose-dependent manner ( $P < 0.05$ ). Moreover, The LDH activity analysis findings indicated that ox-LDL induced significant cytotoxicity relative to the control group. Also, different concentrations of inclisiran markedly inhibited ox-LDL induced cytotoxicity in a dose-dependent manner ( $P < 0.05$ , *Figure 4C*). Taken together, these results

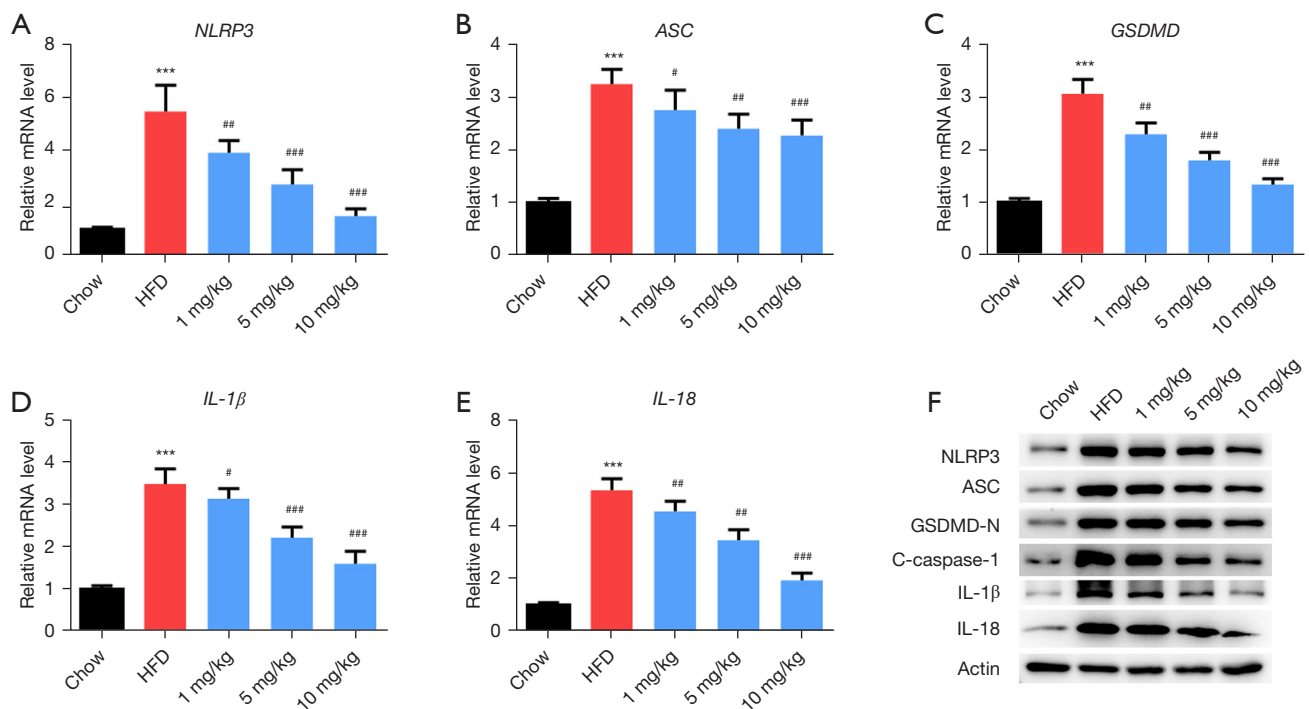


**Figure 3** Inclisiran inhibited pyroptosis in an AS mouse model. (A-E) mRNA levels of *NLRP3*, *ASC*, *GSDMD*, *IL-1β*, and *IL-18* were determined by qRT-PCR. (F) Protein levels of NLRP3, ASC, GSDMD-N, C-caspase-1, IL-1β, and IL-18 were determined by western blot. \*\*\* $P < 0.001$  vs. the chow group. # $P < 0.05$ , ## $P < 0.01$ , and ### $P < 0.001$  vs. the HFD group. HFD, high-fat diet; NLRP3, NOD-like receptor family pyrin domain containing 3; ASC, apoptosis-associated speck-like protein containing a caspase-1 recruitment domain; GSDMD-N, gasdermin-D-N; C-caspase-1, cleaved caspase-1; IL-1β, interleukin-1β; IL-18, interleukin-18; AS, atherosclerosis; qRT-PCR, quantitative real-time polymerase chain reaction.

demonstrate that inclisiran inhibited HUVEC cell death induced by ox-LDL.

#### ***Inclisiran inhibited HUVEC pyroptosis induced by ox-LDL***

As demonstrated in *Figure 5A-5E*, the mRNA levels of *NLRP3*, *ASC*, *GSDMD*, *IL-1β*, and *IL-18* in the ox-LDL group were higher than those in the control group ( $P < 0.05$ ). Meanwhile, compared with the ox-LDL group, inclisiran at different concentrations significantly inhibited *NLRP3*, *ASC*, *GSDMD*, *IL-1β*, and *IL-18* mRNA expression ( $P < 0.05$ ). Furthermore, the western blot results indicated that NLRP3, ASC, GSDMD-N, cleaved caspase-1, IL-1β, and IL-18 protein levels in the ox-LDL group were higher than those in the control group, and different concentrations of inclisiran inhibited the protein expression of NLRP3, ASC, GSDMD-N, cleaved caspase-1, IL-1β, and IL-18 (*Figure 5F*). Collectively, these results indicate that inclisiran inhibited HUVEC pyroptosis induced by ox-LDL.

#### **Discussion**

AS is the main pathological basis of cardiovascular and cerebrovascular disease, and increases the incidence of myocardial infarction, stroke, and other diseases (21,22). Previous studies have shown that PCSK9 not only indirectly regulates blood lipid metabolism but also directly affects AS by participating in regulating lipid accumulation, inflammation, and apoptosis in the blood vessel wall (10,23,24). Therefore, PCSK9 has been identified as an important target for the treatment of AS. Furthermore, new drugs including PCSK9 inhibitors have received increasing attention. Initially, monoclonal antibodies were widely used to reduce the circulating levels of PCSK9. Thus, evolocumab and alirocumab, which are human monoclonal antibodies against PCSK9, have been shown to significantly reduce cardiovascular risk in the context of statin therapy (25,26). As a siRNA targeting PCSK9, inclisiran could replace monoclonal antibodies to reduce the production

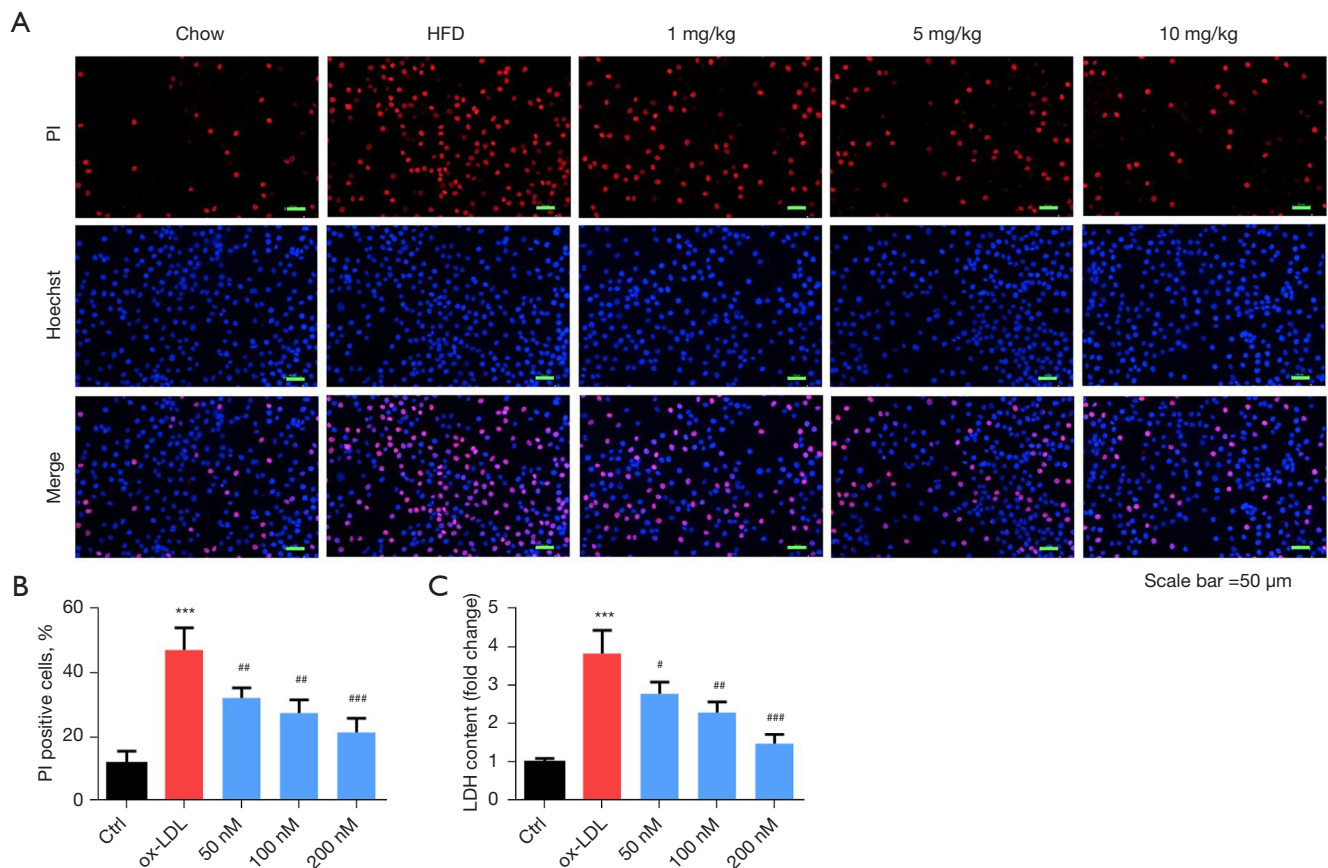


**Figure 4** Inclisiran inhibited HUVEC cell death induced by ox-LDL. (A,B) Cell death was determined by the Hoechst 33342/PI dual-staining assay. Scale bar =50  $\mu$ m. (C) Cytotoxicity was measured by LDH activity analysis. <sup>\*\*\*</sup> $P<0.001$  vs. the control group; <sup>#</sup> $P<0.05$ , <sup>##</sup> $P<0.01$ , and <sup>###</sup> $P<0.001$  vs. the ox-LDL group. HFD, high-fat diet; PI, propidium iodide; LDH, lactate dehydrogenase; ox-LDL, oxidized low-density lipoprotein; HUVEC, human umbilical vein endothelial cell.

of PCSK9 (27). The effect of inclisiran on AS and its mechanism were investigated in the current study.

Most AS models are based on a HFD (28,29). In this study, an AS mouse model was induced by HFD. Studies have shown that lipid metabolism disorder is an important risk factor for AS (30). Dyslipidemia usually refers to the abnormality of the lipid quality and quantity in the plasma, including the increase of TC, TG, and LDL-C, and the decrease of HDL-C (31,32). The deposition of LDL-C on the intima of the arterial wall contributes to plaque formation and AS, restricting blood flow to vital organs, and increasing the risk of atherosclerotic thrombosis and sequelae of AS (33). In the present study, TC, TG, and LDL-C were increased, while HDL-C was decreased in the blood of mice fed with HFD, indicating that model was successfully established. Moreover, we found that inclisiran inhibited the levels of LDL-C, TC, and TG, and increased

the level of HDL-C, which is consistent with a previous study showing that inclisiran markedly reduced the level of LDL-C (27). Collectively, these results demonstrated that inclisiran inhibited blood lipids in mice with AS.

The formation of atheromatous plaques in the arterial intima is basic pathology of AS (34). The progressive increase of AS plaques will result in thickening of the blood vessel walls, narrowing of the blood vessel lumen, and reduced blood supply to the heart (35). In this study, a large number of lipids entered the arterial wall and formed plaques locally, and inclisiran reduced the plaque area in a dose-dependent manner. NLRP3, the most widely studied inflammasome in pyroptosis, is essential for the formation of AS, and its silencing can increase the stability of AS plaques (36). Activation of NLRP3 recruits ASC to promote the activation of caspase-1, resulting in the processing of inflammatory cytokines into mature forms,

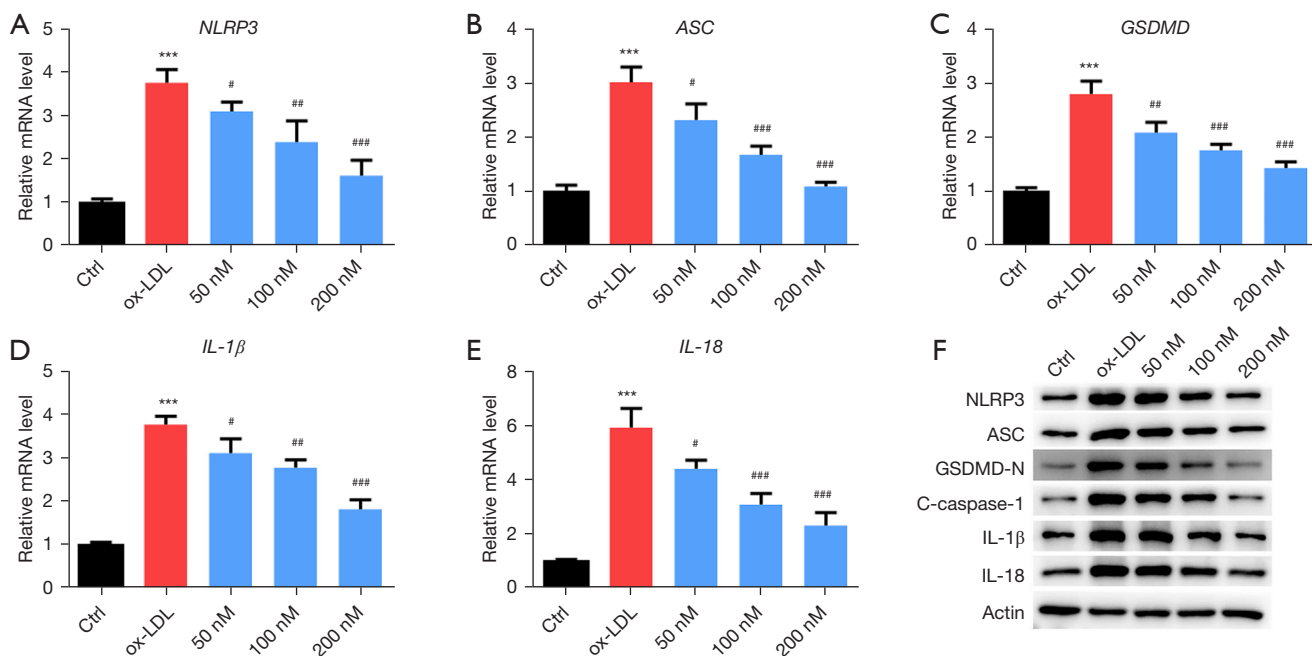


**Figure 5** Inclisiran inhibited HUVEC pyroptosis induced by ox-LDL. (A-E) mRNA levels of *NLRP3*, *ASC*, *GSDMD*, *IL-1β*, and *IL-18* were determined by qRT-PCR. (F) Protein levels of NLRP3, ASC, GSDMD-N, C-caspase-1, IL-1β, and IL-18 were measured by western blot. \*\*\* $P < 0.001$  vs. the control group; # $P < 0.05$ , ## $P < 0.01$ , and ### $P < 0.001$  vs. the ox-LDL group. ox-LDL, oxidized low-density lipoprotein; NLRP3, NOD-like receptor family pyrin domain containing 3; ASC, apoptosis-associated speck-like protein containing a caspase-1 recruitment domain; GSDMD-N, gasdermin-D-N; C-caspase-1, cleaved caspase-1; IL-1β, interleukin-1β; IL-18, interleukin-18; HUVEC, human umbilical vein endothelial cell; qRT-PCR, quantitative real-time polymerase chain reaction.

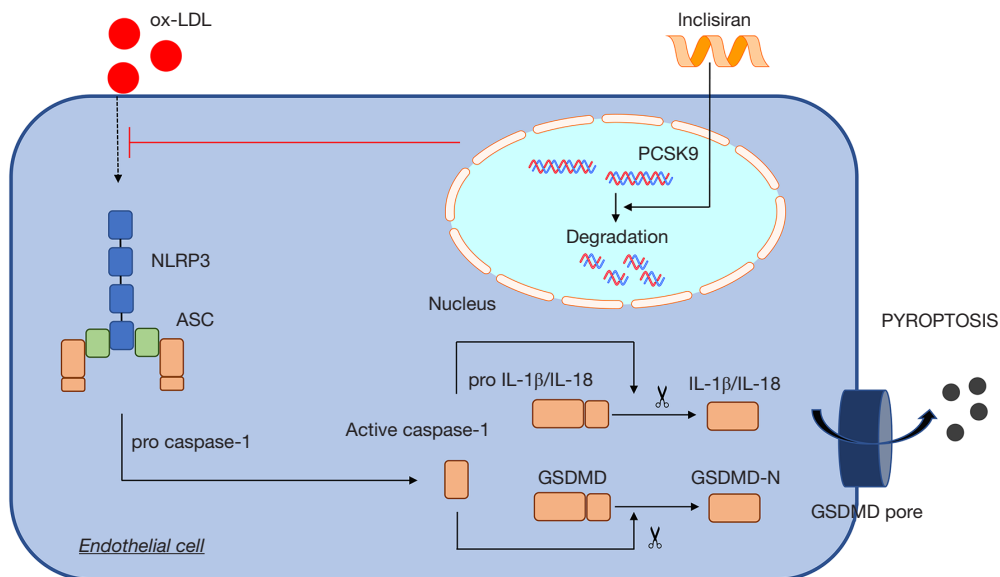


**Figure 6** Schematic diagram of inclisiran exerting its anti-atherosclerotic effects. PCSK9, proprotein convertase subtilisin/kexin type 9; ox-LDL, oxidized low-density lipoprotein; NLRP3, NOD-like receptor family pyrin domain containing 3; ASC, apoptosis-associated speck-like protein containing a caspase-1 recruitment domain; GSDMD-N, gasdermin-D-N; IL-1β, interleukin-1β; IL-18, interleukin-18.



and ultimately leading to pyroptosis (37). In this study, the AS model mice exhibited the characteristics of pyroptosis in aortic ECs, as observed by the increased levels of cleaved caspase-1, NLRP3, ASC, GSDMD-N, IL-1 $\beta$ , and IL-18. Inclisiran inhibited these levels, indicating that the inhibition of EC pyroptosis may be the treatment mechanism of inclisiran in AS.

We further investigated the effect of inclisiran on AS and its mechanism in cell experiments. Ox-LDL, a vital risk factor for AS, participated in the occurrence and development of AS and was used for the establishment of the AS cell models (38). In the present study, a cell model of AS was established via ox-LDL treatment. Inclisiran was found to inhibit cell death and cytotoxicity. Cell death is the basic feature of AS (39). Moreover, we found that inclisiran could significantly inhibit pyroptosis-related proteins in cells, including NLRP3, ASC, GSDMD-N, IL-1 $\beta$ , and IL-18, which is consistent with the results of the mouse model. As shown in *Figure 6*, our results demonstrated that inclisiran exerted anti-atherosclerotic functions mainly by inhibiting NLRP3 activation induced by ox-LDL and then impeding the activation of ASC and caspase-1, thereby hindering the mature morphology of inflammatory cytokines, and ultimately inhibiting EC pyroptosis.

## Conclusions

Inclisiran exerts an anti-atherosclerotic effect, as evidenced by its inhibition of blood lipids, development of AS, and pyroptosis. These findings provide evidence that the PCSK9 inhibitor inclisiran has potential for the treatment of AS via inhibiting cell pyroptosis.

## Acknowledgments

*Funding:* None.

## Footnote

*Reporting Checklist:* The authors have completed the ARRIVE reporting checklist. Available at <https://atm.amegroups.com/article/view/10.21037/atm-22-4652/rc>

*Data Sharing Statement:* Available at <https://atm.amegroups.com/article/view/10.21037/atm-22-4652/dss>

*Conflicts of Interest:* All authors have completed the ICMJE uniform disclosure form (available at <https://atm.amegroups.com/article/view/10.21037/atm-22-4652/coif>).

The authors have no conflicts of interest to declare.

*Ethical Statement:* The authors are accountable for all aspects of the work in ensuring that questions related to the accuracy or integrity of any part of the work are appropriately investigated and resolved. The animal experiments were performed according to the guidelines of the Chinese Ethics Committee for the care and use of animal research and were approved by the Animal Care and Use Committee of Naval Medical University (No. SCXK2021-0910).

*Open Access Statement:* This is an Open Access article distributed in accordance with the Creative Commons Attribution-NonCommercial-NoDerivs 4.0 International License (CC BY-NC-ND 4.0), which permits the non-commercial replication and distribution of the article with the strict proviso that no changes or edits are made and the original work is properly cited (including links to both the formal publication through the relevant DOI and the license). See: <https://creativecommons.org/licenses/by-nc-nd/4.0/>.

## References

1. Libby P. The changing landscape of atherosclerosis. *Nature* 2021;592:524-33.
2. Bułdak Ł. Cardiovascular Diseases-A Focus on Atherosclerosis, Its Prophylaxis, Complications and Recent Advancements in Therapies. *Int J Mol Sci* 2022;23:4695.
3. Pouwer MG, Pieterman EJ, Worms N, et al. Alirocumab, evinacumab, and atorvastatin triple therapy regresses plaque lesions and improves lesion composition in mice. *J Lipid Res* 2020;61:365-75.
4. Padro T, Muñoz-García N, Peña E, et al. Sex Differences and Emerging New Risk Factors for Atherosclerosis and Its Thrombotic Complications. *Curr Pharm Des* 2021;27:3186-97.
5. Xia XD, Peng ZS, Gu HM, et al. Regulation of PCSK9 Expression and Function: Mechanisms and Therapeutic Implications. *Front Cardiovasc Med* 2021;8:764038.
6. Lebeau PF, Byun JH, Platko K, et al. Caffeine blocks SREBP2-induced hepatic PCSK9 expression to enhance LDLR-mediated cholesterol clearance. *Nat Commun* 2022;13:770.
7. Sundararaman SS, Peters LJF, Nazir S, et al. PCSK9 Imperceptibly Affects Chemokine Receptor Expression In Vitro and In Vivo. *Int J Mol Sci* 2021;22:13026.

8. Mazura AD, Ohler A, Storck SE, et al. PCSK9 acts as a key regulator of A $\beta$  clearance across the blood-brain barrier. *Cell Mol Life Sci* 2022;79:212.
9. Arida A, Legaki AI, Kravvariti E, et al. PCSK9/LDLR System and Rheumatoid Arthritis-Related Atherosclerosis. *Front Cardiovasc Med* 2021;8:738764.
10. Punch E, Klein J, Diaba-Nuhoho P, et al. Effects of PCSK9 Targeting: Alleviating Oxidation, Inflammation, and Atherosclerosis. *J Am Heart Assoc* 2022;11:e023328.
11. Ray KK, Landmesser U, Leiter LA, et al. Inclisiran in Patients at High Cardiovascular Risk with Elevated LDL Cholesterol. *N Engl J Med* 2017;376:1430-40.
12. Hadjiphilippou S, Ray KK. PCSK9 inhibition and atherosclerotic cardiovascular disease prevention: does reality match the hype? *Heart* 2017;103:1670-9.
13. Ray KK, Wright RS, Kallend D, et al. Two Phase 3 Trials of Inclisiran in Patients with Elevated LDL Cholesterol. *N Engl J Med* 2020;382:1507-19.
14. Zheng Y, Gardner SE, Clarke MC. Cell death, damage-associated molecular patterns, and sterile inflammation in cardiovascular disease. *Arterioscler Thromb Vasc Biol* 2011;31:2781-6.
15. Zhao J, Jiang P, Guo S, et al. Apoptosis, Autophagy, NETosis, Necroptosis, and Pyroptosis Mediated Programmed Cell Death as Targets for Innovative Therapy in Rheumatoid Arthritis. *Front Immunol* 2021;12:809806.
16. Hou J, Hsu JM, Hung MC. Molecular mechanisms and functions of pyroptosis in inflammation and antitumor immunity. *Mol Cell* 2021;81:4579-90.
17. Peng N, Meng N, Wang S, et al. An activator of mTOR inhibits oxLDL-induced autophagy and apoptosis in vascular endothelial cells and restricts atherosclerosis in apolipoprotein E<sup>-/-</sup> mice. *Sci Rep* 2014;4:5519.
18. Wu X, Zhang H, Qi W, et al. Nicotine promotes atherosclerosis via ROS-NLRP3-mediated endothelial cell pyroptosis. *Cell Death Dis* 2018;9:171.
19. Xing SS, Yang J, Li WJ, et al. Salidroside Decreases Atherosclerosis Plaque Formation via Inhibiting Endothelial Cell Pyroptosis. *Inflammation* 2020;43:433-40.
20. Zhao S, Kang R, Deng T, et al. Comparison of two cannulation methods for assessment of intracavernosal pressure in a rat model. *PLoS One* 2018;13:e0193543.
21. Porsch F, Mallat Z, Binder CJ. Humoral immunity in atherosclerosis and myocardial infarction: from B cells to antibodies. *Cardiovasc Res* 2021;117:2544-62.
22. Knol WG, Budde RPJ, Mahtab EAF, et al. Intimal aortic atherosclerosis in cardiac surgery: surgical strategies to prevent embolic stroke. *Eur J Cardiothorac Surg* 2021;60:1259-67.
23. Seidah NG, Garçon D. Expanding Biology of PCSK9: Roles in Atherosclerosis and Beyond. *Curr Atheroscler Rep* 2022;24:821-30.
24. Keeter WC, Carter NM, Nadler JL, et al. The AAV-PCSK9 murine model of atherosclerosis and metabolic dysfunction. *Eur Heart J Open* 2022;2:oeac028.
25. Sabatine MS, Giugliano RP, Keech AC, et al. Evolocumab and Clinical Outcomes in Patients with Cardiovascular Disease. *N Engl J Med* 2017;376:1713-22.
26. Steg PG, Kumbhani D, Eagle K. Evaluation of cardiovascular outcomes after an acute coronary syndrome during treatment with alirocumab-ODYSSEY OUTCOMES. *Proceedings of the American College of Cardiology Annual Scientific Session (ACC 2018)*, 2018:10-2.
27. Kosmas CE, Muñoz Estrella A, Sourlas A, et al. Inclisiran: A New Promising Agent in the Management of Hypercholesterolemia. *Diseases* 2018;6:63.
28. Haghikia A, Zimmermann F, Schumann P, et al. Propionate attenuates atherosclerosis by immune-dependent regulation of intestinal cholesterol metabolism. *Eur Heart J* 2022;43:518-33.
29. Zhao J, Yang M, Wu J. CXCL16 may be a predisposing factor to atherosclerosis: An animal study. *Mol Med Rep* 2021;24:716.
30. Zhang S, Hong F, Ma C, et al. Hepatic Lipid Metabolism Disorder and Atherosclerosis. *Endocr Metab Immune Disord Drug Targets* 2022;22:590-600.
31. Opoku S, Gan Y, Fu W, et al. Prevalence and risk factors for dyslipidemia among adults in rural and urban China: findings from the China National Stroke Screening and prevention project (CNSSPP). *BMC Public Health* 2019;19:1500.
32. Cheon SY, Cho K. Lipid metabolism, inflammation, and foam cell formation in health and metabolic disorders: targeting mTORC1. *J Mol Med (Berl)* 2021;99:1497-509.
33. Zhang PY. PCSK9 as a therapeutic target for cardiovascular disease. *Exp Ther Med* 2017;13:810-4.
34. Jebari-Benslaiman S, Galicia-García U, Larrea-Sebal A, et al. Pathophysiology of Atherosclerosis. *Int J Mol Sci* 2022;23:3346.
35. Gluvic ZM, Zafirovic SS, Obradovic MM, et al. Hypothyroidism and Risk of Cardiovascular Disease. *Curr Pharm Des* 2022;28:2065-72.
36. Takahashi M. NLRP3 Inflammasome as a Common Denominator of Atherosclerosis and Abdominal Aortic Aneurysm. *Circ J* 2021;85:2129-36.

37. Huang Y, Xu W, Zhou R. NLRP3 inflammasome activation and cell death. *Cell Mol Immunol* 2021;18:2114-27.
38. Bian W, Jing X, Yang Z, et al. Downregulation of LncRNA NORAD promotes Ox-LDL-induced vascular endothelial cell injury and atherosclerosis. *Aging (Albany*

- NY) 2020;12:6385-400.
39. Grootaert MOJ, Moulis M, Roth L, et al. Vascular smooth muscle cell death, autophagy and senescence in atherosclerosis. *Cardiovasc Res* 2018;114:622-34.

(English Language Editor: A. Kassem)

**Cite this article as:** Kong N, Xu Q, Cui W, Feng X, Gao H. PCSK9 inhibitor inclisiran for treating atherosclerosis via regulation of endothelial cell pyroptosis. *Ann Transl Med* 2022;10(22):1205. doi: 10.21037/atm-22-4652